

A Multi-scale Methodology to Assess the Cavitation Erosion Risk on a Twisted Hydrofoil

MARINE 2023

Ziyang Wang^{*,†}, Huaiyu Cheng^{*}, Rickard E. Bensow[†] and Bin Ji^{*}

* State Key Laboratory of Water Resources Engineering and Management, Wuhan University,
No. 8 Donghunan Road, 430072 Wuhan, China
e-mail: zywang96@whu.edu.cn

† Mechanics and Maritime Sciences, Chalmers University of Technology,
41296 Gothenburg, Sweden
e-mail: rickard.bensow@chalmers.se

Corresponding author: Ziyang Wang, zywang96@whu.edu.cn

ABSTRACT

The aim of the current paper is to evaluate the cavitation erosion on a Delft twisted hydrofoil using a coupled Euler-Lagrange methodology. The transport equation modelling approach is introduced to handle the macroscopic liquid-vapor mixture, which is regarded as a homogeneous continuum. The Keller-Herring equation and bubble motion equation are used to track the bubble's dynamics and trajectory. A two-way coupling method is employed to describe the interaction between the mixture and bubbles. A newly developed Lagrangian erosion model is used to assess the cavitation erosion on the hydrofoil. The numerical results are in good agreement with the experimental test data. The statistical results reveal the evolution characteristics of cavitation erosion. The relationship between macroscopic cavitation structure and potential erosion sensitive zone indicates the cavitation erosion intensity at different stages of cloud cavitation. This study contributes to a deeper understanding of the mechanism of cavitation damage from a multi-scale perspective.

Keywords: Cavitation; Cavitation erosion; Euler-Lagrange method; Bubble dynamics

1. INTRODUCTION

Fluid machinery, such as ship propeller and pumped storage power station, is widely used in engineering. Unsteady cavitating flow is a common phenomenon in the operation of fluid machinery, which contains multi-scale turbulent structures and complex phase-change phenomena (Arndt et al., 2000). The development of sheet/cloud cavitation may induce cavitation erosion on the material surface, seriously threatening the normal operation of fluid

machinery. Therefore, it is necessary to conduct the in-depth investigation into the mechanism and characteristics of sheet/cloud cavitation erosion to guide the optimal design.

There is no doubt that paint testing is the most intuitive way to assess the cavitation erosion risk of a design. Knapp (1955) first applied the paint testing method to examine the distribution of cavitation damage on the object's surface. Following his work, many researchers also employed the same method to assess the cavitation erosion on various types of arrangements, such as hydrofoil (Arabnejad et al., 2020), nozzle (Franc, 2009), and blunt body (Jahangir et al., 2021). However, considering the cost and site, the experimental test method has clear limitations. On the other hand, with the development of computer technology, more and more scholars have begun to use computational fluid dynamics (CFD) methods to estimate the cavitation erosion risk. Li et al. (2014) applied the accumulation of the time derivative of pressure and a suitable threshold to evaluate the material erosion risk. Dular and Coutier-Delgosha (2009) proposed a near-wall micro-jet model to evaluate cavitation erosion. Mihatsch et al. (2015) developed a compressible technology to identify high-intensity pressure pulsation on the material surface. Moreover, this method was then applied to assess the cavitation erosion risk in the nozzle (Trummler et al., 2022) and hydrofoil surface (Arabnejad et al., 2020). Schenke and van Terwisga (2019) used the potential energy hypothesis to predict the instantaneous surface impact power of collapsing cavities and then assessed the erosive aggressiveness of cloud cavitation. Recently, Arabnejad et al. (2021) proposed a new cavitation erosion model from the perspective of energy conversion. They considered both the micro-jets and shock waves mechanisms and successfully assessed the cavitation erosion risk in the nozzle. In addition, the Euler-Lagrange method is also introduced to investigate the cavitation erosion. For example, Ochiai et al. (2010) used the near-wall bubble information to calculate the shock pressure released by the Lagrangian bubbles and then assess the cavitation erosion. On the basis his research, Peters and Moctar (2020) and Wang et al. (2022) improved this method and used it to predict the high erosion risk area in the nozzle.

As inspired by the previous study, the current paper aims to use a multi-scale method to systematically assess the cavitation erosion around the Delft twisted hydrofoil. The relationship between the hydrodynamic structures with the cavitation risk is also discussed.

2. NUMERICAL METHODOLOGY

This multi-scale method consists of four parts, the Euler framework, the Lagrange framework, the transition algorithm, and the cavitation erosion assessment. In the Euler framework, large eddy simulation (LES) is introduced to solve the governing equations on the numerical grids. The volume of fluid (VOF) technology is used to identify the vapor-liquid interface. The mass transfer process is simulated by the Schnerr-Sauer model (Schnerr and Sauer, 2001). In the Lagrange framework, the bubbles are tracked using Newton's laws of motion, which considers the virtual mass force, the pressure gradient force, the volume variation force, the buoyancy force, the drag force, and the lift force. The bubble dynamics are described by the Keller-Herring equation. The transition algorithm can realize the conversion between the macroscopic cavity and microscopic bubbles according to their sizes, shape, and relative position. In the

cavitation erosion assessment part, based on the bubble information, the program calculates the impact pressure released by the near-wall bubbles and assesses the cavitation erosion risk on the hydrofoil surface. For details, the reader can refer to our previous studies (Wang et al., 2021, 2022).

3. NUMERICAL SETUP

We considered the unsteady cavitating flow around a Delft twisted hydrofoil, one of the classic cavitation test cases (Cao et al., 2017; Foeth, 2008). As shown in Figure 1, the cross-section is a 2D NACA009 hydrofoil, and the spanwise angle of attack varies from -2° to 9° , reaching a maximum in the middle. The chord length of the hydrofoil, C , is 0.15 m, and the distance between the leading edge of the hydrofoil and the inlet is $2C$. The origin of the coordinate system is set in the middle of the hydrofoil. Similar to the original experiment, the inlet velocity is set to 6.97 m/s, corresponding to a Reynolds number equal to 1.04×10^6 . The outlet pressure is about 29000 Pa to keep the cavitation number $\sigma = 1.07$. The no-slip boundary condition is employed on the hydrofoil surface, and a symmetry plane is used at the tunnel's center. The current work is conducted in the OpenFOAM, and a fixed time step, $\Delta t = 5 \times 10^{-6}$ s, is used to maintain the maximum Courant number less than 1. A set of mesh with 11.4 million nodes is used for the following analysis through the grid independence verification. As shown in Figure 2, The near-surface region is refined to keep the dimensionless wall distance $y^+ < 1$.

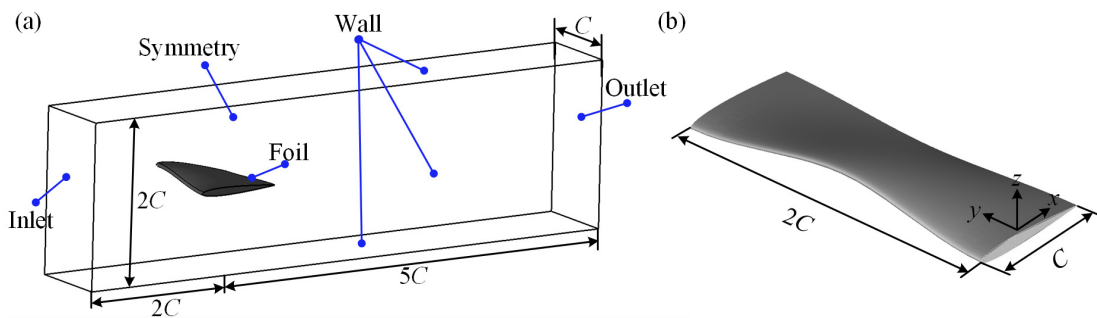


Figure 1. (a) Computational domain, and (b) geometry of the twisted hydrofoil.

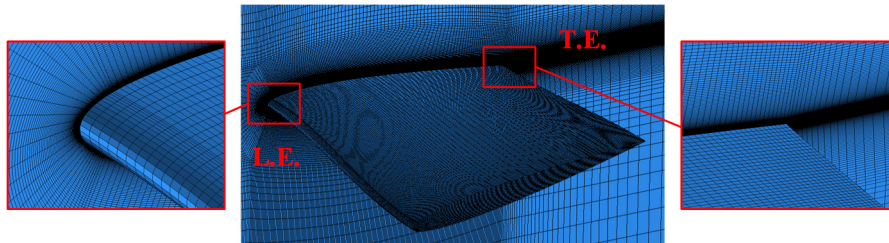


Figure 2. Mesh distribution around the Delft twisted hydrofoil (middle), leading edge (left) and trailing edge (right).

4. RESULT AND DISCUSSION

Fig. 3 compares the experimental data (Cao et al., 2017) and the potential erosion risk area

identified by this Lagrangian erosion method. According to the flow condition, the threshold of the impact pressure is selected as 1 MPa. In the original experimental test, region 1 has the most prominent damage range and the highest intensity. The cavitation erosion damage in regions 2 and 3 appears as isolated points, and their risk is much smaller than in region 1. Fig. 3 (b) shows the calculated potential erosion risk on the Delft hydrofoil surface, and the color represents the impact intensity. The black dashed line visualizes the cavitation erosion area. Fig. 3 (c) further shows the cumulative distribution of the high-impact pressure. It is obvious that the Lagrangian erosion model can overall predict potential cavitation erosion risk areas. As indicated by the black arrow in Fig. 3 (b), some of the impulsive presses occurred at the front of the hydrofoil. Although no apparent cavitation erosion was found in this area in the current experiment, some numerical results gained similar phenomenon (Lei et al., 2021). Meanwhile, in the cavitation erosion experiment around a straight hydrofoil, a strip-shaped damaged area will occur on the leading edge (Arabnejad et al., 2020). Therefore, we believed current calculation results are still reliable. Additionally, as shown by the black dashed arrow in Fig. 3 (b), erosion areas 2 and 3 are connected with erosion area 1. That is, there are two slender erosion areas along the flow direction on the rear part of the hydrofoil surface. Cao et al. (2017) reported that the collapse of the U-shaped cloud produced these two regions.

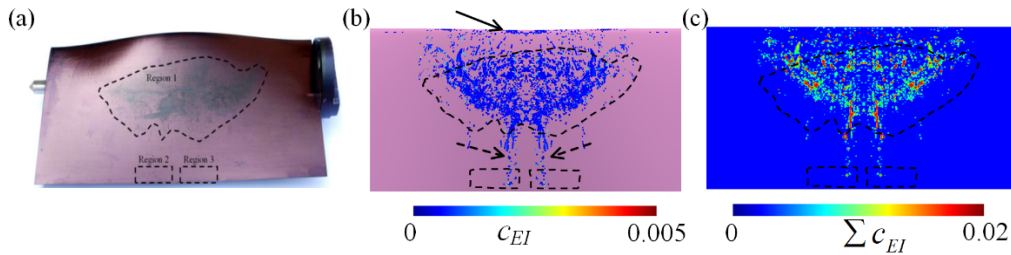


Figure 3. Comparison of (a) experimental results and numerical simulations (b) the detected dimensionless high-pressure impact and (c) cumulative value.

Fig. 4 (a) shows the multi-scale cavitating flow field at six typical instants in one typical cycle. Fig. 4 (b) shows the dimensionless high-impact pressure distribution on the hydrofoil surface at different stages. It is evident that, during stage I-II, the re-entrant jet moves upstream and hits the attached sheet cavity, which causes it to start to break off. The high-impact pressure is mainly concentrated around the sheet cavity closure line. This phenomenon is similar to cavitation erosion on a straight hydrofoil surface (Arabnejad et al., 2020). As shown by the black dashed circle in stage II-III, the re-entrant jet finally cuts off the attached cavity, and a narrow strip region of high erosion risk occurred near the hydrofoil leading edge. When the primary cavity sheds from the surface in the next stage, many microscopic bubbles detach from the cloud edge and travel into the higher-pressure recovery zone, increasing the erosion potential. Note that many aggressive collapse events are generated at this stage, and cavitation erosion risk is highest throughout the cycle. In stage IV-V, the cloud gradually rises and forms into a U-shaped cavity due to the influence of the lift force, while the small-scale bubbles mainly surround it. As shown by the black dashed arrow, the erosion area at the rear presents a strip along the flow direction, which is caused by the collapse of bubbles near the legs of the U-shaped vortex. Compared with the previous stage, in stage V-VI, when the U-shaped structure starts to collapse,

the erosion risk intensity near its leg is also reduced. Compared with the previous stages, the cavitation erosion risk caused by the U-shaped cavity is much smaller than that caused by the primary cavity shedding. In addition, as indicated by the black dashed circle in stage V-VI, the bubble collapse induced by the secondary shedding process is responsible for small-scale, high-intensity erosion damage on the surface, which should be paid much attention in the future.

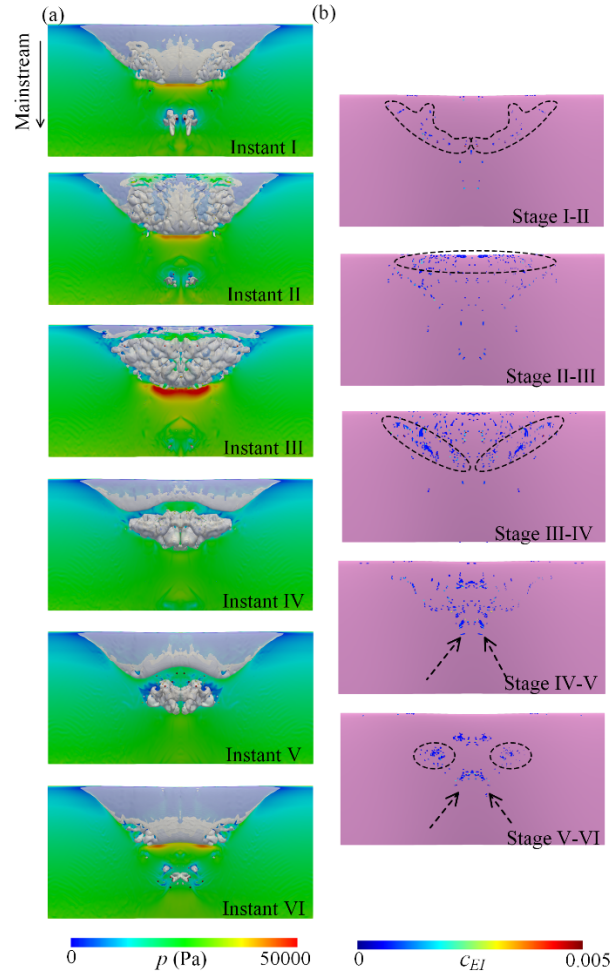


Figure 4. Cavitation characteristics at different stages in a typical cloud cavitation cycle. (a) Multi-scale cavitating flow field and (b) the dimensionless high impact pressure distribution in different stages.

5. CONCLUSION

The multi-scale cavitating flow around the Delft twisted hydrofoil is investigated using a two-way coupling Euler-Lagrange method. A Lagrangian erosion method is introduced to assess the cavitation erosion risk according to the information about the near-wall bubbles. Compared with the experimental paint test, the multi-scale erosion model can precisely identify the high erosion risk region. In addition, the hydrodynamic mechanism of cavitation erosion at different stages is investigated. It is shown that the cavitation erosion risk is the highest during the primary shedding process. The risk of cavitation erosion induced by the U-shaped structure is

minimal, which is appeared as two narrow strips on the rear part of the hydrofoil.

ACKNOWLEDGMENTS

This work was financially supported by the National Natural Science Foundation of China (Project nos. 52176041 and 12102308), and China Scholarship Council (Project no. 202206270064).

REFERENCES

Arabnejad, M.H., Amini, A., Farhat, M., Bensow, R.E., 2020. Hydrodynamic mechanisms of aggressive collapse events in leading edge cavitation. *Journal of Hydrodynamics* 32 (1), 6-19.

Arabnejad, M.H., Svennberg, U., Bensow, R.E., 2021. Numerical assessment of cavitation erosion risk using incompressible simulation of cavitating flows. *Wear* 464-465, 203529.

Arndt, R.E.A., Song, C.C.S., Kjeldsen, M., Keller, A., 2000. Instability of Partial Cavitation: A Numerical/Experimental Approach, In: *Proceedings 23rd Symposium on Naval Hydrodynamics*, Val de Reuil, France.

Cao, Y.T., Peng, X.X., Yan, K., Xu, L.H., Shu, L.W., 2017. A Qualitative Study on the Relationship Between Cavitation Structure and Erosion Region around a 3D Twisted Hydrofoil by Painting Method, 5th International Symposium on Marine Propulsors, Finland.

Dular, M., Coutier-Delgosha, O., 2009. Numerical modelling of cavitation erosion. *International Journal for Numerical methods in fluids* 61 (12), 1388-1410.

Foeth, E.J., 2008. The structure of three-dimensional sheet cavitation. Delft University of Technology, TU Delft.

Franc, J.P., 2009. Incubation time and cavitation erosion rate of work-hardening materials. *Journal of Fluids Engineering* 131, 021303.

Jahangir, S., Ghahramani, E., Neuhauser, M., Bourgeois, S., Bensow, R.E., Poelma, C., 2021. Experimental investigation of cavitation-induced erosion around a surface-mounted bluff body. *Wear* 480-481, 203917.

Knapp, R.T., 1955. Recent investigations of the mechanics of cavitation and cavitation damage. *ASME* 77, 1045-1054.

Lei, T.T., Cheng, H.Y., Ji, B., Peng, X.X., 2021. Numerical assessment of the erosion risk for cavitating twisted hydrofoil by three methods. *Journal of Hydrodynamics* 33 (4), 698-711.

Li, Z.R., Pourquie, M., van Terwisga, T., 2014. Assessment of Cavitation Erosion With a URANS Method. *Journal of Fluids Engineering* 136 (4), 041101.

Mihatsch, M.S., Schmidt, S.J., Adams, N.A., 2015. Cavitation erosion prediction based on analysis of flow dynamics and impact load spectra. *Physics of Fluids* 27 (10), 103302.

Ochiai, N., Iga, Y., Nohmi, M., Ikohagi, T., 2010. Numerical Prediction of Cavitation Erosion Intensity in Cavitating Flows around a Clark Y 11.7% Hydrofoil. *Journal of Fluid Science and Technology* 5 (3), 416-431.

Peters, A., Moctar, O., 2020. Numerical assessment of cavitation-induced erosion using a multi-scale Euler–Lagrange method. *Journal of Fluid Mechanics* 894, A19.

Schenke, S., van Terwisga, T.J.C., 2019. An energy conservative method to predict the erosive aggressiveness of collapsing cavitating structures and cavitating flows from numerical simulations. *International Journal of Multiphase Flow* 111, 200-218.

Schnerr, G.H., Sauer, J., 2001. Physical and numerical modeling of unsteady cavitation dynamics, Fourth International Conference on Multiphase Flow, New Orleans, USA.

Trummler, T., Schmidt, S.J., Adams, N.A., 2022. Numerical prediction of erosion due to a cavitating jet. *Wear* 498-499, 204304.

Wang, Z.Y., Cheng, H.Y., Ji, B., 2021. Euler–Lagrange study of cavitating turbulent flow around a hydrofoil. *Physics of Fluids* 33 (11), 112108.

Wang, Z.Y., Cheng, H.Y., Ji, B., 2022. Numerical prediction of cavitation erosion risk in an axisymmetric nozzle using a multi-scale approach. *Physics of Fluids* 34 (6), 062112.